Two-temperature extension of the HTR solver for hypersonic turbulent flows in thermochemical nonequilibrium

By C. Williams, M. Di Renzo† AND J. Urzay

1. Motivations and Objectives

The Hypersonics Task-Based Research (HTR) solver was originally developed for direct numerical simulations of canonical chemically-reacting compressible turbulent flows in vibrational equilibrium using high-order schemes for spatial discretization, together with both explicit and semi-implicit methods for time integration (Di Renzo *et al.* 2020; Di Renzo & Urzay 2021). This report describes an extension of HTR to compute hypersonic flows at conditions where the characteristic residence time is comparable to the vibrational and chemical relaxation times, thereby providing simulation capabilities for hypersonic flows in thermochemical nonequilibrium.

One way of modeling thermochemical nonequilibrium is the consideration of two temperatures in the formulation, along with an appropriate coupling between dissociation chemistry and vibrational relaxation, as molecules at high vibrational energy levels are more prone to dissociate (Hammerling *et al.* 1959; Treanor & Marrone 1962; Marrone & Treanor 1963). In the two-temperature model considered in the present study, the first temperature T characterizes the translational and rotational energy modes of the gas molecules, while the second temperature T_{ve} describes the extent of vibrational and electronic excitation. In the approach of Park (1990), which is followed here, the dissociation rate constants in air are evaluated at the geometric mean temperature $\sqrt{TT_{ve}}$.

The remainder of this report is structured as follows. A summary of the two-temperature formulation implemented in HTR is provided in Section 2. Relevant numerical aspects are discussed in Section 3. Numerical results from test cases are analyzed in Section 4. Lastly, conclusions are given in Section 5.

2. Formulation

The momentum and species conservation equations, along with the equation of state and constitutive laws for the viscous stress tensor and the diffusion velocity, including all the mathematical notation, are same as those in Di Renzo *et al.* (2020), and therefore symbols will not be redefined here. In contrast, the conservation equation for the specific stagnation internal energy e_0 (including chemical energy) is revised here as

$$\frac{\partial(\rho e_0)}{\partial t} + \nabla\cdot(\rho h_0 \mathbf{u}) = \nabla\cdot\left(\overline{\overline{\boldsymbol{\tau}}}\mathbf{u} + \lambda_{tr}\nabla T + \lambda_{ve}\nabla T_{ve} - \sum_{i=1}^{N_s}\rho_i \boldsymbol{V_i} h_i\right). \tag{2.1}$$

In this formulation, λ_{tr} is the thermal conductivity of the rotational and translational modes, and λ_{ve} is the thermal conductivity corresponding to the vibrational and elec-

† CERFACS, France

tronic excitation energy modes, both calculated via Eucken's relation (Vincenti & Kruger 1965). The specific internal energy e accounts for the different energy modes as

$$e = \sum_{i=1}^{N_s} Y_i \left(e_{tr,i} + e_{v,i} + e_{e,i} + h^0_{i,f} \right), \tag{2.2}$$

with $h^0_{i,f}$ being the enthalpy of formation of species i at zero K. Correspondingly, h_i is the partial specific enthalpy of species i defined as

$$h_i = \sum_{i=1}^{N_s} Y_i \left(\mathrm{R}^0 T/\mathcal{M}_i + e_{tr,i} + e_{v,i} + e_{e,i} + h^0_{i,f} \right). \tag{2.3}$$

In these expressions, $e_{v,i}$, and $e_{e,i}$ are the specific internal energies of vibration and and electronic excitation of species i, respectively. Similarly, $e_{tr,i}$ represents the sum of translational and rotational internal energies of of species i.

The rotational and translational modes are taken to be fully excited, with the molecular species being treated as rigid rotors, namely

$$e_{tr,i} = (3/2)\mathrm{R}^0 T/\mathcal{M}_i + \mathcal{V}\mathrm{R}^0 T/\mathcal{M}_i. \tag{2.4}$$

In this notation, the prefactor $\mathcal{V}$ is equal to 0 and 1 for monoatomic and diatomic species, respectively. The computation of the vibrational energy is based on the treatment of molecules as quantum harmonic oscillators, with both the vibrational and electronic-excitation energy modes characterized by T_{ve} as

$$e_{v,i} = \frac{\mathcal{V}\Theta_{v,i}\mathrm{R}^0/\mathcal{M}_i}{\exp(\Theta_{v,i}/T_{ve}) - 1}, \tag{2.5}$$

$$e_{e,i} = \frac{\mathrm{R}^0 T_{ve}^2}{\mathcal{M}_i} \frac{\partial}{\partial T_{ve}} \left\{ \ln \left[\sum_j g_{i,j} \exp(-\Theta_{el,i,j}/T_{ve}) \right] \right\}. \tag{2.6}$$

In this formulation, $\Theta_{v,i}$ is the characteristic vibrational temperature of species i, while $\Theta_{el,i,j}$, and $g_{i,j}$ are, respectively, the characteristic temperature and degeneracy of the electronic energy level j for species i.

In this two-temperature approach, the sum of the vibrational and electronic-excitation specific internal energies

$$e_{ve} = \sum_{i=1}^{N_s} Y_i e_{ve,i} = \sum_{i=1}^{N_s} Y_i (e_{v,i} + e_{e,i}) \tag{2.7}$$

is described by the conservation equation (Gnoffo *et al.* 1989)

$$\frac{\partial(\rho e_{ve})}{\partial t} + \nabla\cdot(\rho e_{ve}\mathbf{u}) = \nabla\cdot\left(\lambda_{ve}\nabla T_{ve} - \sum_{i=1}^{N_s} \rho_i \boldsymbol{V_i} e_{ve,i} \right) + \sum_{i=1}^{N_s} \rho_i \frac{e^*_{v,i} - e_{v,i}}{\tau_i} + \dot{w}_{ve}. \tag{2.8}$$

In Eq. (2.8), the second term on the right-hand side corresponds to exchange between the vibrational and translational energy modes (Landau & Teller 1936), where $e^\star_{v,i}$ is the equilibrium vibrational internal energy calculated using expression (2.5) evaluated at the translational-rotational temperature T. Similarly, τ_i is a vibrational-relaxation time of

species i given by (Park 1990)

$$\tau_i = \tau_i^P + \left(\sum_{j=1}^{N_s} \frac{X_j}{\tau_{ij}^{MW}} \right)^{-1}. \tag{2.9}$$

In this expression, τ_{ij}^{MW} is the vibrational-relaxation time proposed by Millikan & White (1963), namely

$$\tau_{ij}^{MW} = \frac{1.01394 \times 10^{-3}}{P} \exp\left[a_{ij} \left(T^{-1/3} - b_{ij} \right) \right] \qquad [\mathrm{s}], \tag{2.10}$$

which corresponds to molecule i colliding with species j, where P is in atm, T is in K, and the empirical constants a_{ij} and b_{ij} are taken from Park (1993). Additionally, τ_i^P represents the high-temperature correction given by (Park 1990)

$$\tau_i^P = \left[n \sigma_v \sqrt{(8 \mathrm{R}^0 T / \pi \mathcal{M}_i)} \right]^{-1}, \tag{2.11}$$

where n is the number density, and σ_v is the effective cross section (Park 1993)

$$\sigma_v = 3 \times 10^{-21} \left(50,000/T \right)^2 \quad [\mathrm{m}^2]. \tag{2.12}$$

As the enthalpies considered here are insufficient to yield significant ionization, the air is modeled as a mixture of N_2, O_2, NO, N, and O. The first seven electronic energy levels are used for each species, with the characteristic temperature and degeneracy data taken from the NIST databases for atomic† and diatomic species‡.

The chemical reactions considered include three dissociation (forward) or recombination (backward) reactions for each of the molecular species, as well as two shuffle reactions [see Eqs. (R1)-(R5) in Di Renzo *et al.* (2020) for details]. The forward rate constants of each one of the three dissociation reactions are given by

$$k_f(\sqrt{T T_{ve}}) = A \ \left(T T_{ve} \right)^{m/2} \exp\left(- \frac{E_a}{\mathrm{R}^0 \sqrt{T T_{ve}}} \right), \tag{2.13}$$

with A, m, and E_a being the Arrhenius parameters listed in Park (1990). In contrast, the recombination (backward) rate constants are evaluated at the translational-rotational temperature as

$$k_b(T) = k_f(T) / K_{eq}(T), \tag{2.14}$$

where K_{eq} is the chemical equilibrium constant calculated using the polynomial form

$$K_{eq} = \exp\left(\frac{\mathcal{A}_1}{Z} + \mathcal{A}_2 + \mathcal{A}_3 \log Z + \mathcal{A}_4 Z + \mathcal{A}_5 Z^2 \right), \tag{2.15}$$

with $Z = 10^4/T$. The numerical values of the coefficients $\mathcal{A}_i$ are given in Park (1990) for each of the reactions.

Two different models for the dissociation/vibrational-excitation coupling term $\dot{w}_{ve}$ in Eq. (2.8) are considered here, namely the preferential-dissociation model (Sharma *et al.* 1992)

$$\dot{w}_{ve} = 0.3 \sum_{i=1}^{N_s} \dot{w}_i \tilde{D}_i, \tag{2.16}$$

† Accessed 2021: `https://physics.nist.gov/PhysRefData/ASD/levels_form.html`
‡ Accessed 2021: `https://webbook.nist.gov/chemistry/`

and the non-preferential dissociation model (Candler & MacCormack 1991)

$$\dot{w}_{ve} = \sum_{i=1}^{N_s} \dot{w}_i e_{v,i}. \tag{2.17}$$

In this formulation, $\tilde{D}_i$ and $\dot{w}_i$ are, respectively, the specific dissociation energy and mass production rate per unit time and volume of species i, with $\tilde{D}_i = 0$ for monoatomic species. Equation (2.16) accounts for preferential dissociation from the highest vibrational energy levels by taking the vibrational energy lost per dissociation as being a significant portion of the molecule's overall dissociation energy. In contrast, Eq. (2.17) models a non-preferential dissociation process by assuming the vibrational energy lost per dissociation is, on average, equivalent to the mean vibrational energy.

3. Numerical aspects of the extension

The first step in the high-order flux-reconstruction procedure implemented in HTR entails projecting the vectors of conserved variables and fluxes into characteristic space using the Roe-averaged left eigenvector matrices. Once in characteristic space, a local Lax-Friedrichs flux splitting is employed to calculate the respective flux functions. The positive and negative flux functions at the cell interfaces are reconstructed using a sixth-order TENO scheme (Fu *et al.* 2016), and the flux at the cell interface is taken as the average of these positive and negative flux functions. Thereafter, the fluxes are projected back to physical space using the right eigenvectors of the Roe-averaged flux Jacobian (Di Renzo *et al.* 2020).

The projections to and from characteristic space in the high-order reconstruction procedure motivate the derivation of the Roe-averaged flux Jacobians and their eigendecomposition provided below for hypersonic flows in thermochemical nonequilibrium. Relevant early work on this topic is reported in Grossman & Cinnella (1990) and Shuen *et al.* (1990). In particular, Grossman & Cinnella (1990) derived a Roe scheme accounting for chemical and vibrational nonequilibrium, allowing each molecular species to be treated as a harmonic oscillator at a distinct vibrational temperature. Subsequently, the flux-difference splitting of Shuen *et al.* (1990) considered Roe averaging for flows in chemical nonequilibrium and vibrational equilibrium, and introduced a useful pressure-correction procedure to enforce consistency of the Roe-averaged pressure derivatives that participate in the calculation of the Roe-averaged flux Jacobian.

By extending the Roe-averaging approach and pressure-correction procedure of Shuen *et al.* (1990), the present study derives a Roe-averaged state that accounts for both chemical and vibrational nonequilibrium, while also enforcing consistency of the Roe-averaged pressure derivatives. The resulting formulation holds for any two-temperature model, thermochemical properties, and vibrational-relaxation rates.

3.1. *Roe averaging*

For inviscid hypersonic flows in thermochemical nonequilibrium, the Euler equations can be written in conservative form as

$$\frac{\partial \mathbf{C}}{\partial t} + \frac{\partial \mathbf{F}(\mathbf{C})}{\partial x} + \frac{\partial \mathbf{G}(\mathbf{C})}{\partial y} + \frac{\partial \mathbf{H}(\mathbf{C})}{\partial z} = 0, \tag{3.1}$$

where $\mathbf{C}$ is the vector of conserved variables

$$\mathbf{C} = [\rho_1, \dots \rho_N, \rho u, \rho v, \rho w, \rho e_0, \rho e_{ve}]^{\mathrm{T}}, \tag{3.2}$$

and

$$\mathbf{F}(\mathbf{C}) = \begin{bmatrix} \rho_1 u \\ \vdots \\ \rho_N u \\ \rho u u + P \\ \rho u v \\ \rho u w \\ \rho u h_0 \\ \rho u e_{ve} \end{bmatrix}, \quad \mathbf{G}(\mathbf{C}) = \begin{bmatrix} \rho_1 v \\ \vdots \\ \rho_N v \\ \rho v u \\ \rho v v + P \\ \rho v w \\ \rho v h_0 \\ \rho v e_{ve} \end{bmatrix}, \quad \mathbf{H}(\mathbf{C}) = \begin{bmatrix} \rho_1 w \\ \vdots \\ \rho_N w \\ \rho w u \\ \rho w v \\ \rho w w + P \\ \rho w h_0 \\ \rho w e_{ve} \end{bmatrix} \tag{3.3}$$

are the Euler fluxes. In order to calculate the flux Jacobians, however, the derivatives of pressure with respect to thermodynamic variables must be determined. By allowing for thermochemical nonequilibrium, the thermodynamic state of the gas depends not only on the set of partial densities and the internal energy, but also on the vibrational-electronic energy. As such, the pressure is defined as $P = P(\rho_i, e, e_{ve})$ and its exact differential is

$$dP = \sum_{i=1}^{N_s} P_{\rho_i} d\rho_i + P_e de + P_{e_{ve}} de_{ve}, \tag{3.4}$$

where P_{ρ_i} is the partial derivative of pressure with respect to the partial density of species i, P_e is the partial derivative of pressure with respect to the internal energy, and $P_{e_{ve}}$ is the partial derivative of pressure with respect to the vibrational-electronic energy. Under the assumption of an ideal gas, these partial derivatives with respect to thermodynamic variables can be expressed as

$$P_{\rho_i} = \left(\frac{\partial P}{\partial \rho_i}\right)_{\rho_j, j\neq i, e, e_{ve}} = \frac{\mathrm{R}^0 T}{\mathcal{M}_i} + \frac{\mathrm{R}^0}{c_v^{tr}\overline{\mathcal{M}}}\left(e - e_{ve} + e_{ve,i} - e_i\right), \tag{3.5}$$

where $\overline{\mathcal{M}}$ is the mean molecular mass and c_v^{tr} is the translational-rotational specific heat of the mixture. Likewise, the remaining partial derivatives of pressure with respect to the thermodynamic variables are

$$P_e = \left(\frac{\partial P}{\partial e}\right)_{\rho_i, e_{ve}} = \frac{\rho \mathrm{R}^0}{c_v^{tr}\overline{\mathcal{M}}}, \qquad P_{e_{ve}} = \left(\frac{\partial P}{\partial e_{ve}}\right)_{\rho_i, e} = -\frac{\rho \mathrm{R}^0}{c_v^{tr}\overline{\mathcal{M}}}. \tag{3.6}$$

In order to construct the Roe-averaged flux Jacobians, the Roe-averaging operator

$$\Phi(\mathcal{Y}) = \frac{\sqrt{\rho_R}\mathcal{Y}_R + \sqrt{\rho_L}\mathcal{Y}_L}{\sqrt{\rho_R} + \sqrt{\rho_L}} \tag{3.7}$$

is defined for a flow variable $\mathcal{Y}$, where the subscripts R and L denote quantities to the right and left of a cell interface. Using Eq. (3.7), the Roe-averaged flow variables are defined as

$$\begin{gathered} \widehat{\rho} = \sqrt{\rho_R \rho_L}, \quad \widehat{Y}_i = \Phi(Y_i), \quad \widehat{u} = \Phi(u), \quad \widehat{v} = \Phi(v), \quad \widehat{w} = \Phi(w), \\ \widehat{e}_0 = \Phi(e_0), \quad \widehat{e}_{ve} = \Phi(e_{ve}), \quad \widehat{h}_0 = \Phi(h_0). \end{gathered} \tag{3.8}$$

Likewise, in order for the Roe-averaged flux Jacobian to satisfy its own definition,

$$\Delta F = \widehat{(dF/dC)}\Delta C, \tag{3.9}$$

where $\Delta() = ()_R - ()_L$, the Roe-averaged velocity is defined in accordance with

$$\widehat{\mathcal{U}^2} = \widehat{u}^2 + \widehat{v}^2 + \widehat{w}^2. \tag{3.10}$$

3.2. *Roe-averaged flux Jacobian and eigenvector matrices*

Based on the considerations above, the Roe-averaged flux Jacobian in the x-direction can be expressed as

$$\widehat{\frac{d\mathbf{F}}{d\mathbf{C}}} = \begin{bmatrix} \widehat{u}(1-\widehat{Y}_1) & \dots & -\widehat{u}\widehat{Y}_1 & \widehat{Y}_1 & 0 & 0 & 0 & 0 \\ \vdots & \ddots & \vdots & \vdots & \vdots & \vdots & \vdots & \vdots \\ -\widehat{u}\widehat{Y}_{N_s} & \dots & \widehat{u}(1-\widehat{Y}_{N_s}) & \widehat{Y}_{N_s} & 0 & 0 & 0 & 0 \\ \widehat{\mathcal{G}}_1 - \widehat{u}^2 & \dots & \widehat{\mathcal{G}}_{N_s} - \widehat{u}^2 & \left(2 - \frac{\widehat{P}_e}{\widehat{\rho}}\right)\widehat{u} & -\frac{\widehat{P}_e}{\widehat{\rho}}\widehat{v} & -\frac{\widehat{P}_e}{\widehat{\rho}}\widehat{w} & \frac{\widehat{P}_e}{\widehat{\rho}} & \frac{\widehat{P}_{e_{ve}}}{\widehat{\rho}} \\ -\widehat{u}\widehat{v} & \dots & -\widehat{u}\widehat{v} & \widehat{v} & \widehat{u} & 0 & 0 & 0 \\ -\widehat{u}\widehat{w} & \dots & -\widehat{u}\widehat{w} & \widehat{w} & 0 & \widehat{u} & 0 & 0 \\ \widehat{u}\left(\widehat{\mathcal{G}}_1 - \widehat{h}_0\right) & \dots & \widehat{u}\left(\widehat{\mathcal{G}}_{N_s} - \widehat{h}_0\right) & \widehat{h}_0 - \frac{\widehat{P}_e}{\widehat{\rho}}\widehat{u}^2 & -\frac{\widehat{P}_e}{\widehat{\rho}}\widehat{u}\widehat{v} & -\frac{\widehat{P}_e}{\widehat{\rho}}\widehat{u}\widehat{w} & \left(1 + \frac{\widehat{P}_e}{\widehat{\rho}}\right)\widehat{u} & \frac{\widehat{P}_{e_{ve}}}{\widehat{\rho}}\widehat{u} \\ -\widehat{u}\widehat{e}_{ve} & \dots & -\widehat{u}\widehat{e}_{ve} & \widehat{e}_{ve} & 0 & 0 & 0 & \widehat{u} \end{bmatrix}, \tag{3.11}$$

with

$$\widehat{\mathcal{G}}_i = \frac{\widehat{P}_e}{\widehat{\rho}}\left(\frac{\widehat{\mathcal{U}^2}}{2} - \widehat{e}\right) + \widehat{P}_{\rho_i} - \frac{\widehat{P}_{e_{ve}}}{\widehat{\rho}}\widehat{e}_{ve} \tag{3.12}$$

for $i = 1, 2, \dots N_s$. The eigenvalues of the flux Jacobian matrix are $\lambda_i = [\widehat{u}, \dots, \widehat{u}, \widehat{u} + \widehat{a}, \widehat{u} - \widehat{a}, \widehat{u}]$, with the eigenvalue $\widehat{u}$ having a multiplicity of $N_s + 3$. The corresponding matrix of right eigenvectors can then be expressed as

$$\widehat{\mathbf{K}}_{\mathbf{F}} = \begin{bmatrix} 1/\widehat{a}^2 & \dots & 0 & 0 & 0 & \widehat{Y}_1/2\widehat{a}^2 & \widehat{Y}_1/2\widehat{a}^2 & 0 \\ \vdots & \ddots & \vdots & \vdots & \vdots & \vdots & \vdots & \vdots \\ 0 & \dots & 1/\widehat{a}^2 & 0 & 0 & \widehat{Y}_N/2\widehat{a}^2 & \widehat{Y}_N/2\widehat{a}^2 & 0 \\ \widehat{u}/\widehat{a}^2 & \dots & \widehat{u}/\widehat{a}^2 & 0 & 0 & (\widehat{u}+\widehat{a})/2\widehat{a}^2 & (\widehat{u}-\widehat{a})/2\widehat{a}^2 & 0 \\ \widehat{v}/\widehat{a}^2 & \dots & \widehat{v}/\widehat{a}^2 & 1 & 0 & \widehat{v}/2\widehat{a}^2 & \widehat{v}/2\widehat{a}^2 & 0 \\ \widehat{w}/\widehat{a}^2 & \dots & \widehat{w}/\widehat{a}^2 & 0 & 1 & \widehat{w}/2\widehat{a}^2 & \widehat{w}/2\widehat{a}^2 & 0 \\ \widehat{\mathcal{F}}_i/\widehat{a}^2 & \dots & \widehat{\mathcal{F}}_{N_s}/\widehat{a}^2 & \widehat{v} & \widehat{w} & (\widehat{h}_0 + \widehat{a}\widehat{u})/2\widehat{a}^2 & (\widehat{h}_0 - \widehat{a}\widehat{u})/2\widehat{a}^2 & 1/\widehat{a}^2 \\ 0 & \dots & 0 & 0 & 0 & \widehat{e}_{ve}/2\widehat{a}^2 & \widehat{e}_{ve}/2\widehat{a}^2 & 1/\widehat{a}^2 \end{bmatrix}, \tag{3.13}$$

where the Roe-averaged speed of sound $\widehat{a}$ satisfies

$$\widehat{a}^2 = \sum_{i=1}^{N_s} \widehat{P}_{\rho_i}\widehat{Y}_i + \frac{\widehat{p_e}}{\widehat{\rho}}\left(\widehat{h}_0 - \widehat{e} - \frac{\widehat{\mathcal{U}^2}}{2}\right), \tag{3.14}$$

and $\widehat{\mathcal{F}}_i$ is an auxiliary variable defined as

$$\widehat{\mathcal{F}}_i = \left(\widehat{e} + \frac{\widehat{\mathcal{U}^2}}{2} - \widehat{\rho}\frac{\widehat{P}_{\rho i}}{\widehat{P}_e} + \frac{\widehat{P}_{e_{ve}}}{\widehat{P}_e}\widehat{e}_{ve}\right) \tag{3.15}$$

for $i = 1, 2, \dots N_s$. Correspondingly, the matrix of left eigenvectors is

$$\widehat{\mathbf{K}}_{\mathbf{F}}^{-1} = \begin{bmatrix} \widehat{a}^2 - \widehat{Y}_1\widehat{\mathcal{G}}_1 & \dots & -\widehat{Y}_1\widehat{\mathcal{G}}_{N_s} & \frac{\widehat{P}_e}{\widehat{\rho}}\widehat{Y}_1\widehat{u} & \frac{\widehat{P}_e}{\widehat{\rho}}\widehat{Y}_1\widehat{v} & \frac{\widehat{P}_e}{\widehat{\rho}}\widehat{Y}_1\widehat{w} & -\frac{\widehat{P}_e}{\widehat{\rho}}\widehat{Y}_1 & -\frac{\widehat{P}_{e_{ve}}}{\widehat{\rho}}\widehat{Y}_1 \\ \vdots & \ddots & \vdots & \vdots & \vdots & \vdots & \vdots & \vdots \\ -\widehat{Y}_{N_s}\widehat{\mathcal{G}}_1 & \dots & \widehat{a}^2 - \widehat{Y}_{N_s}\widehat{\mathcal{G}}_{N_s} & \frac{\widehat{P}_e}{\widehat{\rho}}\widehat{Y}_N\widehat{u} & \frac{\widehat{P}_e}{\widehat{\rho}}\widehat{Y}_N\widehat{v} & \frac{\widehat{P}_e}{\widehat{\rho}}\widehat{Y}_N\widehat{w} & -\frac{\widehat{P}_e}{\widehat{\rho}}\widehat{Y}_N & -\frac{\widehat{P}_{e_{ve}}}{\widehat{\rho}}\widehat{Y}_N \\ -\widehat{v} & \dots & -\widehat{v} & 0 & 1 & 0 & 0 & 0 \\ -\widehat{w} & \dots & -\widehat{w} & 0 & 0 & 1 & 0 & 0 \\ \widehat{\mathcal{G}}_1 - \widehat{u}\widehat{a} & \dots & \widehat{\mathcal{G}}_{N_s} - \widehat{u}\widehat{a} & \widehat{a} - \frac{\widehat{P}_e}{\widehat{\rho}}\widehat{u} & -\frac{\widehat{P}_e}{\widehat{\rho}}\widehat{v} & -\frac{\widehat{P}_e}{\widehat{\rho}}\widehat{w} & \frac{\widehat{P}_e}{\widehat{\rho}} & \frac{\widehat{P}_{e_{ve}}}{\widehat{\rho}} \\ \widehat{\mathcal{G}}_1 + \widehat{u}\widehat{a} & \dots & \widehat{\mathcal{G}}_{N_s} + \widehat{u}\widehat{a} & -\widehat{a} - \frac{\widehat{P}_e}{\widehat{\rho}}\widehat{u} & -\frac{\widehat{P}_e}{\widehat{\rho}}\widehat{v} & -\frac{\widehat{P}_e}{\widehat{\rho}}\widehat{w} & \frac{\widehat{P}_e}{\widehat{\rho}} & \frac{\widehat{P}_{e_{ve}}}{\widehat{\rho}} \\ -\widehat{\mathcal{G}}_1\widehat{e}_{ve} & \dots & -\widehat{\mathcal{G}}_{N_s}\widehat{e}_{ve} & \frac{\widehat{P}_e}{\widehat{\rho}}\widehat{u}\widehat{e}_{ve} & \frac{\widehat{P}_e}{\widehat{\rho}}\widehat{v}\widehat{e}_{ve} & \frac{\widehat{P}_e}{\widehat{\rho}}\widehat{w}\widehat{e}_{ve} & -\frac{\widehat{P}_e}{\widehat{\rho}}\widehat{e}_{ve} & \widehat{a}^2 - \frac{\widehat{P}_{e_{ve}}}{\widehat{\rho}}\widehat{e}_{ve} \end{bmatrix}. \tag{3.16}$$

An Appendix is included in this report with expressions for the Roe-averaged flux Jacobians in the y- and z-directions, along with their matrices of right and left eigenvectors.

3.3. *Pressure-correction procedure*

The averaged partial derivatives of pressure appearing in the preceding matrices are enforced to satisfy the relation

$$\Delta P = \widehat{P}_{e_{ve}}\Delta e_{ve} + \widehat{P}_e\Delta e + \sum_{i=1}^{N_s}\widehat{P}_{\rho_i}\Delta\rho_i. \tag{3.17}$$

Extending the pressure-correction procedure of Shuen *et al.* (1990), the Roe-averaged partial derivatives of the pressure are given by

$$\widehat{P}_e = \left(\overline{P}_e\Delta e + \omega_e\delta P\right)/\Delta e, \quad \widehat{P}_{e_{ve}} = \left(\overline{P}_{e_{ve}}\Delta e_{ve} + \omega_{e_{ve}}\delta P\right)/\Delta e_{ve},$$
$$\widehat{P}_{\rho_i} = \left(\overline{P}_{\rho_i}\Delta\rho_i + \omega_{\rho_i}\delta P\right)/\Delta\rho_i, \tag{3.18}$$

for $i = 1, 2, \dots N_s$. In Eq. (3.18), δP in is defined as

$$\delta P = \Delta P - \left(\overline{P}_{e_{ve}}\Delta e_{ve} + \overline{P}_e\Delta e + \sum_{i=1}^{N_s}\overline{P}_{\rho_i}\Delta\rho_i\right). \tag{3.19}$$

In these expressions, the partial derivatives $\overline{P}_e$, $\overline{P}_{e_{ve}}$, and $\overline{P}_{\rho_i}$ are calculated by evaluating Eqs. (3.5) and (3.6) in terms of the set of Roe-averaged variables defined in Eq. (3.8). Likewise, the correction weights ω_e, $\omega_{e_{ve}}$, and ω_{ρ_i} are given by

$$\omega_e = \left(\overline{P}_e\Delta e\right)^2 \Big/ \left[\left(\overline{P}_e\Delta e\right)^2 + \left(\overline{P}_{e_{ve}}\Delta e_{ve}\right)^2 + \sum_{i=1}^{N_s}\left(\overline{P}_{\rho_i}\Delta\rho_i\right)^2\right],$$
$$\omega_{e_{ve}} = \left(\overline{P}_{e_{ve}}\Delta e_{ve}\right)^2 \Big/ \left[\left(\overline{P}_e\Delta e\right)^2 + \left(\overline{P}_{e_{ve}}\Delta e_{ve}\right)^2 + \sum_{i=1}^{N_s}\left(\overline{P}_{\rho_i}\Delta\rho_i\right)^2\right],$$
$$\omega_{\rho_i} = \left(\overline{P}_e\Delta\rho_i\right)^2 \Big/ \left[\left(\overline{P}_e\Delta e\right)^2 + \left(\overline{P}_{e_{ve}}\Delta e_{ve}\right)^2 + \sum_{i=1}^{N_s}\left(\overline{P}_{\rho_i}\Delta\rho_i\right)^2\right], \tag{3.20}$$

for $i = 1, 2 \dots N_s$.

4. Test cases

This section focuses on simulation results of benchmark cases. The implementation of the relaxation terms is tested for homogeneous baths of gas molecules, while the high-order flux reconstruction procedure is tested for a model shock tube.

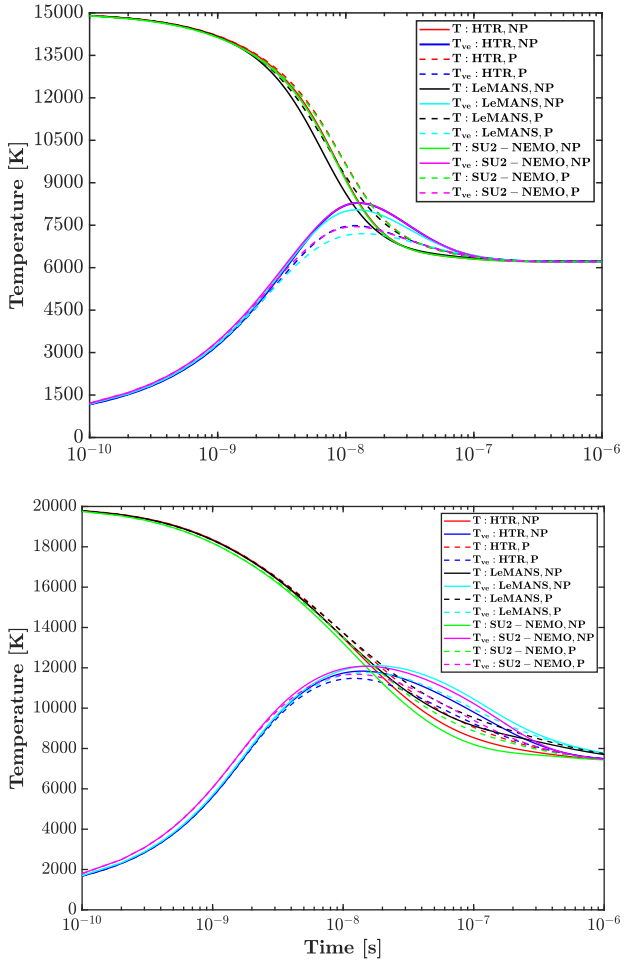

FIGURE 1. Dissociation/vibrational-relaxation coupling in air (top panel) and pure-nitrogen (bottom panel) homogeneous baths. The acronyms P and NP refer, respectively, to preferential and non-preferential dissociation models described in Section 2.

4.1. *Dissociation/vibrational-relaxation coupling in a homogeneous bath of gas molecules*

Homogeneous baths of air and pure nitrogen undergoing vibrational relaxation coupled with dissociation are considered in order to verify some aspects of the implementation of the two-temperature formulation described in Section 2. For air, the initial conditions are $T = 15,000$ K, $T_{ve} = 300$ K, $P = 20.42$ atm, $Y_{\mathrm{N}_2} = 0.767$ and $Y_{\mathrm{O}_2} = 0.233$. Meanwhile for the pure nitrogen case, the initial conditions are: $T = 20,000$ K, $T_{ve} = 300$ K, $P = 27.25$ atm, and $Y_{\mathrm{N}_2} = 1$.

As shown in Figure 1, the time histories of T and T_{ve} computed with HTR closely match the reference data. The reference results are comprised of computations performed with the SU2-NEMO solver (Maier *et al.* 2021), which makes use of the Mutation++ library for thermochemical modeling (Scoggins *et al.* 2020), as well as computations performed with the LeMANS solver (Scalabrin 2007; Gimelshein *et al.* 2021). The agreement between HTR and SU2-NEMO is particularly evident for both preferential and non-preferential

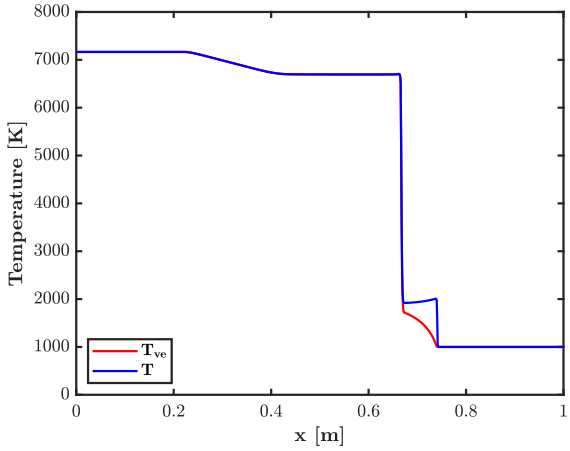

FIGURE 2. Instantaneous spatial distribution of temperatures in a model shock tube.

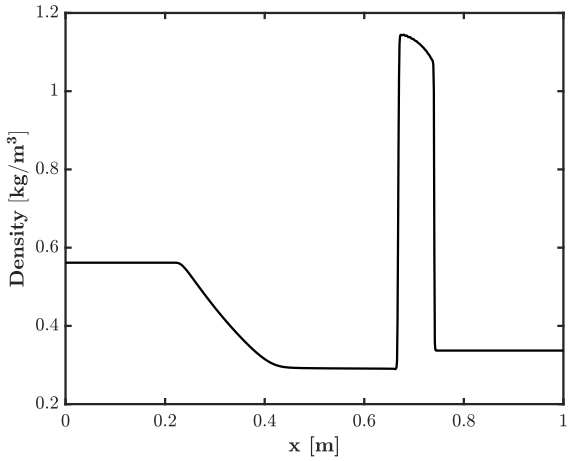

FIGURE 3. Instantaneous spatial distribution of density in a model shock tube.

dissociation models in the case of the air mixture. The small disparities between the results predicted by each code are expected because of the different models employed for computing thermochemical properties and source terms.

4.2. *Dissociation/vibrational-relaxation coupling in a model shock tube*

As confirmation of the shock-capturing capabilities of this flux-reconstruction procedure, the instantaneous spatial distribution of temperatures obtained from a numerical simulation of a one-dimensional shock tube is provided in Figure 2. In this test case, the shock tube is initially divided into two sections, with discontinuities in the primitive variables present at the center of the domain, representing the presence of a diaphragm. The temperature in the left section is initially $12,000$ K, while the temperature to the right of the diaphragm is initially 1000 K; the mixture is uniformly initialized as pure molecular nitrogen in both sections. Initially, the pressure is 2 MPa to the left of the diaphragm, while the right section is initialized with a pressure of 100 kPa. The domain

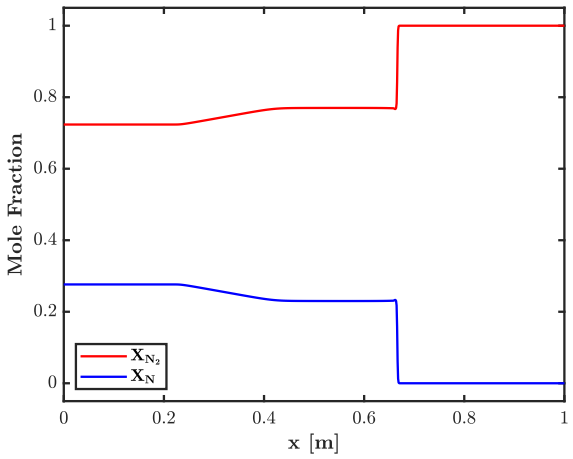

FIGURE 4. Instantaneous spatial distribution of molar fractions in a model shock tube.

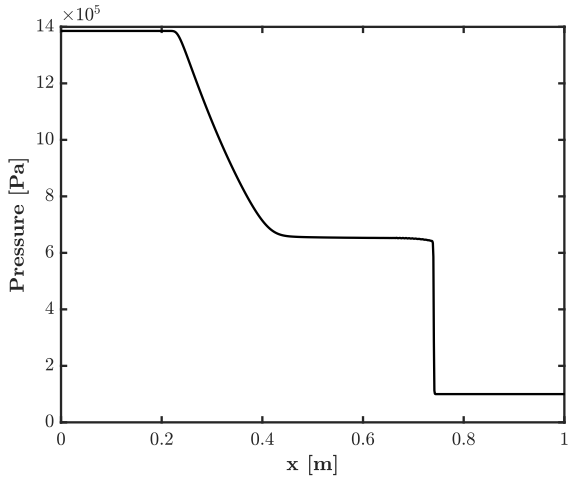

FIGURE 5. Instantaneous spatial distribution of pressure in a model shock tube.

is 1.0 m in length in the x-direction, discretized using 1000 points. Equation (2.16) is used to describe the dissociation/vibrational-relaxation coupling term.

The flow field in the shock tube can be characterized as follows. The high temperatures and pressures in the driver section induce significant dissociation of the molecular nitrogen while the pressure jump in the center of the shock tube produces a rightward-traveling shock, together with an associated expansion region and two contact discontinuities. Containing the temperature profiles at $t = 156$ μs, Figure 2 demonstrates the presence of the shock, expansion, contact discontinuities, and vibrational-relaxation region in the numerical solution. The numerical solution realizes the expected behavior in the post-shock region, with the translational-rotational temperature exhibiting a jump across the shock wave while the vibrational-electronic temperature remains frozen across the shock prior to relaxing behind the discontinuity. Likewise, Figure 3 demonstrates the increase in density associated with the vibrational relaxation process between $x = 0.74$ m and $x = 0.67$ m, bounded by the shock and contact discontinuity. Furthermore, Figure 4 shows that a sig-

nificant fraction of the molecular species has dissociated in the high-temperature region, whereas Figure 5 establishes the presence of the shock and expansion waves. Therefore, the numerical solution is not only consistent with expectation, but also demonstrates the ability of this high-order flux-reconstruction procedure to simulate shocks, expansions, and contact discontinuities, along with the associated post-shock relaxation regions.

5. Conclusions

The HTR solver has been extended to study the interaction between turbulence and nonequilibrium thermochemical processes in hypersonic flows. The formulation includes a two-temperature approach with coupling between air dissociation and vibrational relaxation. The Roe flux-difference-splitting methodology and pressure-correction procedure of Shuen *et al.* (1990) have been extended to account for thermochemical nonequilibrium in a two-temperature framework, and the Roe-averaged flux Jacobians have been employed in a novel high-order flux reconstruction. Relevant parts of the implementation have been verified by comparing simulation results of dissociation coupled with vibrational relaxation in air and pure nitrogen homogeneous baths. The augmented shock-capturing capabilities have been assessed with numerical simulations of a model shock tube subject to dissociation/vibrational-relaxation coupling in pure molecular nitrogen.

Acknowledgments

This investigation was funded by the Advanced Simulation and Computing (ASC) program of the US Department of Energy's National Nuclear Security Administration (NNSA) via the PSAAP-III Center at Stanford, Grant No. DE-NA0002373. C.W. was funded by a Stanford School of Engineering Graduate Fellowship. The authors are grateful to Dr. Jonathan Wang and Prof. Marco Panesi for useful discussions.

Appendix. Expressions for the Roe-averaged flux Jacobians and eigenvector matrices in the y- and z-directions

The Roe-averaged flux Jacobian in the y-direction is

$$\widehat{\frac{d\mathbf{G}}{d\mathbf{C}}} = \begin{bmatrix} \widehat{v}(1-\widehat{Y}_1) & \dots & -\widehat{v}\widehat{Y}_1 & 0 & \widehat{Y}_1 & 0 & 0 & 0 \\ \vdots & \ddots & \vdots & \vdots & \vdots & \vdots & \vdots & \vdots \\ -\widehat{v}\widehat{Y}_N & \dots & \widehat{v}(1-\widehat{Y}_N) & 0 & \widehat{Y}_N & 0 & 0 & 0 \\ -\widehat{v}\widehat{u} & \dots & -\widehat{v}\widehat{u} & \widehat{v} & \widehat{u} & 0 & 0 & 0 \\ \widehat{\mathcal{G}}_1 - \widehat{v}^2 & \dots & \widehat{\mathcal{G}}_{N_s} - \widehat{v}^2 & -\frac{\widehat{P}_e}{\widehat{\rho}}\widehat{u} & (2-\frac{\widehat{P}_e}{\widehat{\rho}})\widehat{v} & -\frac{\widehat{P}_e}{\widehat{\rho}}\widehat{w} & \frac{\widehat{P}_e}{\widehat{\rho}} & \frac{\widehat{P}_{e_{ve}}}{\widehat{\rho}} \\ -\widehat{v}\widehat{w} & \dots & -\widehat{v}\widehat{w} & 0 & \widehat{w} & \widehat{v} & 0 & 0 \\ \widehat{v}\left(\widehat{\mathcal{G}}_1 - \widehat{h}_0\right) & \dots & \widehat{v}\left(\widehat{\mathcal{G}}_{N_s} - \widehat{h}_0\right) & -\frac{\widehat{P}_e}{\widehat{\rho}}\widehat{v}\widehat{u} & \widehat{h}_0 - \frac{\widehat{P}_e}{\widehat{\rho}}\widehat{v}^2 & -\frac{\widehat{P}_e}{\widehat{\rho}}\widehat{v}\widehat{w} & \left(1+\frac{\widehat{P}_e}{\widehat{\rho}}\right)\widehat{v} & \frac{\widehat{P}_{e_{ve}}}{\widehat{\rho}}\widehat{v} \\ -\widehat{v}\widehat{e}_{ve} & \dots & -\widehat{v}\widehat{e}_{ve} & 0 & \widehat{e}_{ve} & 0 & 0 & \widehat{v} \end{bmatrix},$$

whereas the matrices of right and left eigenvectors are

$$\widehat{\mathbf{K}}_{\mathbf{G}} = \begin{bmatrix} 1/\widehat{a}^2 & \dots & 0 & 0 & 0 & \widehat{Y}_1/2\widehat{a}^2 & \widehat{Y}_1/2\widehat{a}^2 & 0 \\ \vdots & \ddots & \vdots & \vdots & \vdots & \vdots & \vdots & \vdots \\ 0 & \dots & 1/\widehat{a}^2 & 0 & 0 & \widehat{Y}_N/2\widehat{a}^2 & \widehat{Y}_N/2\widehat{a}^2 & 0 \\ \widehat{u}/\widehat{a}^2 & \dots & \widehat{u}/\widehat{a}^2 & 0 & 1 & \widehat{u}/2\widehat{a}^2 & \widehat{u}/2\widehat{a}^2 & 0 \\ \widehat{v}/\widehat{a}^2 & \dots & \widehat{v}/\widehat{a}^2 & 0 & 0 & (\widehat{v}+\widehat{a})/2\widehat{a}^2 & (\widehat{v}-\widehat{a})/2\widehat{a}^2 & 0 \\ \widehat{w}/\widehat{a}^2 & \dots & \widehat{w}/\widehat{a}^2 & 1 & 0 & \widehat{w}/2\widehat{a}^2 & \widehat{w}/2\widehat{a}^2 & 0 \\ \widehat{\mathcal{F}}_1/\widehat{a}^2 & \dots & \widehat{\mathcal{F}}_{N_s}/\widehat{a}^2 & \widehat{w} & \widehat{u} & (\widehat{h}_0+\widehat{a}\widehat{v})/2\widehat{a}^2 & (\widehat{h}_0-\widehat{a}\widehat{v})/2\widehat{a}^2 & 1/\widehat{a}^2 \\ 0 & \dots & 0 & 0 & 0 & \widehat{e}_{ve}/2\widehat{a}^2 & \widehat{e}_{ve}/2\widehat{a}^2 & 1/\widehat{a}^2 \end{bmatrix},$$

and

$$\widehat{\mathbf{K}}_{\mathbf{G}}^{-1} = \begin{bmatrix} \widehat{a}^2 - \widehat{Y}_1\widehat{\mathcal{G}}_1 & \dots & -\widehat{Y}_1\widehat{\mathcal{G}}_{N_s} & \frac{\widehat{P}_e}{\widehat{\rho}}\widehat{Y}_1\widehat{u} & \frac{\widehat{P}_e}{\widehat{\rho}}\widehat{Y}_1\widehat{v} & \frac{\widehat{P}_e}{\widehat{\rho}}\widehat{Y}_1\widehat{w} & -\frac{\widehat{P}_e}{\widehat{\rho}}\widehat{Y}_1 & -\frac{\widehat{P}_{e_{ve}}}{\widehat{\rho}}\widehat{Y}_1 \\ \vdots & \ddots & \vdots & \vdots & \vdots & \vdots & \vdots & \vdots \\ -\widehat{Y}_N\widehat{\mathcal{G}}_1 & \dots & \widehat{a}^2 - \widehat{Y}_N\widehat{\mathcal{G}}_{N_s} & \frac{\widehat{P}_e}{\widehat{\rho}}\widehat{Y}_N\widehat{u} & \frac{\widehat{P}_e}{\widehat{\rho}}\widehat{Y}_N\widehat{v} & \frac{\widehat{P}_e}{\widehat{\rho}}\widehat{Y}_N\widehat{w} & -\frac{\widehat{P}_e}{\widehat{\rho}}\widehat{Y}_N & -\frac{\widehat{P}_{e_{ve}}}{\widehat{\rho}}\widehat{Y}_N \\ -\widehat{w} & \dots & -\widehat{w} & 0 & 0 & 1 & 0 & 0 \\ -\widehat{u} & \dots & -\widehat{u} & 1 & 0 & 0 & 0 & 0 \\ \widehat{\mathcal{G}}_1 - \widehat{v}\widehat{a} & \dots & \widehat{\mathcal{G}}_{N_s} - \widehat{v}\widehat{a} & -\frac{\widehat{P}_e}{\widehat{\rho}}\widehat{u} & \widehat{a} - \frac{\widehat{P}_e}{\widehat{\rho}}\widehat{v} & -\frac{\widehat{P}_e}{\widehat{\rho}}\widehat{w} & \frac{\widehat{P}_e}{\widehat{\rho}} & \frac{\widehat{P}_{e_{ve}}}{\widehat{\rho}} \\ \widehat{\mathcal{G}}_1 + \widehat{v}\widehat{a} & \dots & \widehat{\mathcal{G}}_{N_s} + \widehat{v}\widehat{a} & -\frac{\widehat{P}_e}{\widehat{\rho}}\widehat{u} & -\widehat{a} - \frac{\widehat{P}_e}{\widehat{\rho}}\widehat{v} & -\frac{\widehat{P}_e}{\widehat{\rho}}\widehat{w} & \frac{\widehat{P}_e}{\widehat{\rho}} & \frac{\widehat{P}_{e_{ve}}}{\widehat{\rho}} \\ -\widehat{\mathcal{G}}_1\widehat{e}_{ve} & \dots & -\widehat{\mathcal{G}}_{N_s}\widehat{e}_{ve} & \frac{\widehat{P}_e}{\widehat{\rho}}\widehat{u}\widehat{e}_{ve} & \frac{\widehat{P}_e}{\widehat{\rho}}\widehat{v}\widehat{e}_{ve} & \frac{\widehat{P}_e}{\widehat{\rho}}\widehat{w}\widehat{e}_{ve} & -\frac{\widehat{P}_e}{\widehat{\rho}}\widehat{e}_{ve} & \widehat{a}^2 - \frac{\widehat{P}_{e_{ve}}}{\widehat{\rho}}\widehat{e}_{ve} \end{bmatrix},$$

respectively. Similarly, the Roe-averaged flux Jacobian in the z-direction is

$$\widehat{\frac{d\mathbf{H}}{d\mathbf{C}}} = \begin{bmatrix} \widehat{w}(1-\widehat{Y}_1) & \dots & -\widehat{w}\widehat{Y}_1 & 0 & 0 & \widehat{Y}_1 & 0 & 0 \\ \vdots & \ddots & \vdots & \vdots & \vdots & \vdots & \vdots & \vdots \\ -\widehat{w}\widehat{Y}_N & \dots & \widehat{w}(1-\widehat{Y}_N) & 0 & 0 & \widehat{Y}_N & 0 & 0 \\ -\widehat{w}\widehat{u} & \dots & -\widehat{w}\widehat{u} & \widehat{w} & 0 & \widehat{u} & 0 & 0 \\ -\widehat{w}\widehat{v} & \dots & -\widehat{w}\widehat{v} & 0 & \widehat{w} & \widehat{v} & 0 & 0 \\ \widehat{\mathcal{G}}_1 - \widehat{w}^2 & \dots & \widehat{\mathcal{G}}_{N_s} - \widehat{w}^2 & -\frac{\widehat{P}_e}{\widehat{\rho}}\widehat{u} & -\frac{\widehat{P}_e}{\widehat{\rho}}\widehat{v} & (2-\frac{\widehat{P}_e}{\widehat{\rho}})\widehat{w} & \frac{\widehat{P}_e}{\widehat{\rho}} & \frac{\widehat{P}_{e_{ve}}}{\widehat{\rho}} \\ \widehat{w}\left(\widehat{\mathcal{G}}_1 - \widehat{h}_0\right) & \dots & \widehat{w}\left(\widehat{\mathcal{G}}_{N_s} - \widehat{h}_0\right) & -\frac{\widehat{P}_e}{\widehat{\rho}}\widehat{w}\widehat{u} & -\frac{\widehat{P}_e}{\widehat{\rho}}\widehat{w}\widehat{v} & \widehat{h}_0 - \frac{\widehat{P}_e}{\widehat{\rho}}\widehat{w}^2 & (1+\frac{\widehat{P}_e}{\widehat{\rho}})\widehat{w} & \frac{\widehat{P}_{e_{ve}}}{\widehat{\rho}}\widehat{w} \\ -\widehat{w}\widehat{e}_{ve} & \dots & -\widehat{w}\widehat{e}_{ve} & 0 & 0 & \widehat{e}_{ve} & 0 & \widehat{w} \end{bmatrix},$$

whereas the matrices of right and left eigenvectors are

$$\widehat{\mathbf{K}}_{\mathbf{H}} = \begin{bmatrix} 1/\widehat{a}^2 & \dots & 0 & 0 & 0 & \widehat{Y}_1/2\widehat{a}^2 & \widehat{Y}_1/2\widehat{a}^2 & 0 \\ \vdots & \ddots & \vdots & \vdots & \vdots & \vdots & \vdots & \vdots \\ 0 & \dots & 1/\widehat{a}^2 & 0 & 0 & \widehat{Y}_N/2\widehat{a}^2 & \widehat{Y}_N/2\widehat{a}^2 & 0 \\ \widehat{u}/\widehat{a}^2 & \dots & \widehat{u}/\widehat{a}^2 & 1 & 0 & \widehat{u}/2\widehat{a}^2 & \widehat{u}/2\widehat{a}^2 & 0 \\ \widehat{v}/\widehat{a}^2 & \dots & \widehat{v}/\widehat{a}^2 & 0 & 1 & \widehat{v}/2\widehat{a}^2 & \widehat{v}/2\widehat{a}^2 & 0 \\ \widehat{w}/\widehat{a}^2 & \dots & \widehat{w}/\widehat{a}^2 & 0 & 0 & (\widehat{w}+\widehat{a})/2\widehat{a}^2 & (\widehat{w}-\widehat{a})/2\widehat{a}^2 & 0 \\ \widehat{\mathcal{F}}_1/\widehat{a}^2 & \dots & \widehat{\mathcal{F}}_{N_s}/\widehat{a}^2 & \widehat{u} & \widehat{v} & (\widehat{h}_0 + \widehat{w}\widehat{a})/2\widehat{a}^2 & (\widehat{h}_0 - \widehat{w}\widehat{a})/2\widehat{a}^2 & 1/\widehat{a}^2 \\ 0 & \dots & 0 & 0 & 0 & \widehat{e}_{ve}/2\widehat{a}^2 & \widehat{e}_{ve}/2\widehat{a}^2 & 1/\widehat{a}^2 \end{bmatrix}$$

and

$$\widehat{\mathbf{K}}_{\mathbf{H}}^{-1} = \begin{bmatrix} \widehat{a}^2 - \widehat{Y}_1\widehat{\mathcal{G}}_1 & \dots & -\widehat{Y}_1\widehat{\mathcal{G}}_{N_s} & \frac{\widehat{P}_e}{\widehat{\rho}}\widehat{Y}_1\widehat{u} & \frac{\widehat{P}_e}{\widehat{\rho}}\widehat{Y}_1\widehat{v} & \frac{\widehat{P}_e}{\widehat{\rho}}\widehat{Y}_1\widehat{w} & -\frac{\widehat{P}_e}{\widehat{\rho}}\widehat{Y}_1 & -\frac{\widehat{P}_{e_{ve}}}{\widehat{\rho}}\widehat{Y}_1 \\ \vdots & \ddots & \vdots & \vdots & \vdots & \vdots & \vdots & \vdots \\ -\widehat{Y}_{N_s}\widehat{\mathcal{G}}_1 & \dots & \widehat{a}^2 - \widehat{Y}_{N_s}\widehat{\mathcal{G}}_{N_s} & \frac{\widehat{P}_e}{\widehat{\rho}}\widehat{Y}_{N_s}\widehat{u} & \frac{\widehat{P}_e}{\widehat{\rho}}\widehat{Y}_{N_s}\widehat{v} & \frac{\widehat{P}_e}{\widehat{\rho}}\widehat{Y}_N\widehat{w} & -\frac{\widehat{P}_e}{\widehat{\rho}}\widehat{Y}_{N_s} & -\frac{\widehat{P}_{e_{ve}}}{\widehat{\rho}}\widehat{Y}_N \\ -\widehat{u} & \dots & -\widehat{u} & 1 & 0 & 0 & 0 & 0 \\ -\widehat{v} & \dots & -\widehat{v} & 0 & 1 & 0 & 0 & 0 \\ \widehat{\mathcal{G}}_1 - \widehat{w}\widehat{a} & \dots & \widehat{\mathcal{G}}_{N_s} - \widehat{w}\widehat{a} & -\frac{\widehat{P}_e}{\widehat{\rho}}\widehat{u} & -\frac{\widehat{P}_e}{\widehat{\rho}}\widehat{v} & \widehat{a} - \frac{\widehat{P}_e}{\widehat{\rho}}\widehat{w} & \frac{\widehat{P}_e}{\widehat{\rho}} & \frac{\widehat{P}_{e_{ve}}}{\widehat{\rho}} \\ \widehat{\mathcal{G}}_1 + \widehat{w}\widehat{a} & \dots & \widehat{\mathcal{G}}_{N_s} + \widehat{w}\widehat{a} & -\frac{\widehat{P}_e}{\widehat{\rho}}\widehat{u} & -\frac{\widehat{P}_e}{\widehat{\rho}}\widehat{v} & -\widehat{a} - \frac{\widehat{P}_e}{\widehat{\rho}}\widehat{w} & \frac{\widehat{P}_e}{\widehat{\rho}} & \frac{\widehat{P}_{e_{ve}}}{\widehat{\rho}} \\ -\widehat{\mathcal{G}}_1\widehat{e}_{ve} & \dots & -\widehat{\mathcal{G}}_{N_s}\widehat{e}_{ve} & \frac{\widehat{P}_e}{\widehat{\rho}}\widehat{u}\widehat{e}_{ve} & \frac{\widehat{P}_e}{\widehat{\rho}}\widehat{v}\widehat{e}_{ve} & \frac{\widehat{P}_e}{\widehat{\rho}}\widehat{w}\widehat{e}_{ve} & -\frac{\widehat{P}_e}{\widehat{\rho}}\widehat{e}_{ve} & \widehat{a}^2 - \frac{\widehat{P}_{e_{ve}}}{\widehat{\rho}}\widehat{e}_{ve} \end{bmatrix},$$

respectively.

REFERENCES

CANDLER, G. V. & MACCORMACK, R. W. 1991 Computation of weakly ionized hypersonic flows in thermochemical nonequilibrium. *J. Thermophys. Heat Trans.* **5**, 266–273.

Di Renzo, M., Fu, L. & Urzay, J. 2020 HTR solver: An open-source exascale-oriented task-based multi-GPU high-order code for hypersonic aerothermodynamics. *Comput. Phys. Comm.* **255**, 107262.

Di Renzo, M. & Urzay, J. 2021 Direct numerical simulation of a hypersonic transitional boundary layer at suborbital enthalpies. *J. Fluid Mech.* **912**, A29.

Fu, L. & Hu, X. Y. & Adams, N. A. 2016 A family of high-order targeted ENO schemes for compressible-fluid simulations. *J. Comput. Phys.* **305**, 333-359.

Gimelshein, S., Wysong, I., Fangman, A., Andrienko, D., Kunova, O., Kustova, E., Garbacz, C., Fossati, M. & Hanquist, K. 2021 Kinetic and continuum modeling of high temperature relaxation of O2 and N2 binary mixtures. *J. Thermophys. Heat Trans.* (In Press).

Hammerling, P., Teare, J. D. & Kivel, B. 1959 Theory of radiation from luminous shock waves in nitrogen. *Phys. Fluids* **2**, 422–426.

Landau, L. V. & Teller, E. 1936 Zur theorie der schalldispersion. *Phys. Z. Sow.* **10**, 34-43.

Gnoffo, P. A., Gupta, R. N. & Shinn, J. L. 1989 Conservation equations and physical models for hypersonic air flows in thermal and chemical nonequilibrium. NASA TP #2867.

Grossman, B., & Cinnella, P. 1990 Flux-split algorithms for flows with non-equilibrium chemistry and vibrational relaxation. *J. Comp. Phys.* **88**, 131–168.

Maier, W. T., Needels, J. T., Garbacz, C., Morgado, F., Alonso, J. J. & Fossati, M. 2021 SU2-NEMO: An open-source framework for high-Mach nonequilibrium multi-species flows. *Aerosp.* **8** 193-222.

Marrone, P. V. & Treanor, C. E. 1963 Chemical relaxation with preferential dissociation from excited vibrational levels. *Phys. Fluids* **6**, 1215–1221.

Millikan, R. C. & White, D. R. 1963 Systematics of vibrational relaxation. *J. Chem. Phys.* **39**, 3209–3213.

Park, C. 1990 *Nonequilibrium Hypersonic Aerothermodynamics*. Wiley.

Park, C. 1993 Review of chemical-kinetic problems of future Nasa missions: 1 - Earth entries. *J. Thermophys. Heat Trans.* **7**, 385–398.

Scalabrin, L. C. 2007 *Numerical Simulation of Weakly Ionized Hypersonic Flow Over Reentry Capsules.* PhD Thesis, University of Michigan.

Scoggins, J. B., Leroy, V., Bellas-Chatzigeorgis, G., Dias, B. & Magin, T. E. 2020 Mutation++: Multicomponent thermodynamic and transport properties for ionized gases in C++. *SoftwareX* **12**, 100575.

Sharma, S. P., Huo, W. M. & Park, C. 1992 Rate parameters for coupled vibration-dissociation in a generalized ssh approximation. *J. Thermophys. Heat Trans.* **6**, 9–21.

Shuen, J.-S., Liou, M.-S. & Leer, B. V. 1990 Inviscid flux-splitting algorithms for real gases with non-equilibrium chemistry. *J. Comp. Phys.* **90**, 371–395.

Treanor, C. E. & Marrone, P. V. 1962 Effect of dissociation on the rate of vibrational relaxation. *Phys. Fluids* **5**, 1022–1026.

Vincenti, W. G. & Kruger C. H. 1965 *Introduction to Physical Gas Dynamics*. Wiley.